

# 6-Gingerol suppresses cell viability, migration and invasion via inhibiting EMT, and inducing autophagy and ferroptosis in LPS-stimulated and LPS-unstimulated prostate cancer cells

CHI-MING LIU<sup>1\*</sup>, LIJIE AN<sup>1,2\*</sup>, ZHENGPING WU<sup>3</sup>, AI-JUN OUYANG<sup>4</sup>, MENGQIAO SU<sup>1,2</sup>,  
ZICHEN SHAO<sup>1,2</sup>, YI LIN<sup>3</sup>, XIAOYU LIU<sup>3</sup> and YINJIE JIANG<sup>1</sup>

<sup>1</sup>School of Medicine; <sup>2</sup>College of Chemistry and Bio-engineering; <sup>3</sup>School of Aesthetic Medicine, Yichun University, Yichun, Jiangxi 336000; <sup>4</sup>Department of Pharmacy, The First Affiliated Hospital of Nanchang University, Nanchang, Jiangxi 330006, P.R. China

Received January 29, 2022; Accepted March 31, 2022

DOI: 10.3892/ol.2022.13307

**Abstract.** 6-Gingerol is a bioactive compound isolated from *Zingiber officinale*. 6-Gingerol has been shown to have anticancer effects in numerous types of cancer cell. The mechanisms underlying the anticancer effect of 6-Gingerol in prostate cancer requires investigation. In the present study, the effect on cell viability of 6-Gingerol on LNCaP, PC3 and DU145 prostate cancer cells were determined using the MTT and colony formation assays. 6-Gingerol significantly inhibited cell migration, adhesion and invasion in LPS-stimulated and LPS-unstimulated prostate cancer cells. Furthermore, these changes were accompanied by alterations in the protein expression levels of epithelial-mesenchymal transition biomarkers, including E-cadherin, N-cadherin, Vimentin and zonula occludens-1. 6-Gingerol also induced autophagy by significantly increasing LC3B-II and Beclin-1 protein expression levels in prostate cancer cells. Combining 6-Gingerol with LY294002, an autophagy inhibitor, significantly increased cell survival in DU145 cells. Furthermore, 6-Gingerol significantly decreased the protein expression levels of glutathione (GSH) peroxidase 4 and nuclear factor erythroid 2-related factor 2 in prostate cancer cells. Reactive oxygen species (ROS) levels were significantly increased but GSH levels were decreased following 6-Gingerol treatment in prostate cancer cells. Co-treatment with the ferroptosis inhibitor, ferrostatin-1, significantly increased cell viability and significantly decreased ROS levels in 6-Gingerol-treated

cells. These results suggested that 6-Gingerol may have inhibited prostate cell cancer viability via the regulation of autophagy and ferroptosis. In addition, 6-Gingerol inhibited cell migration, adhesion and invasion via the regulation of EMT-related protein expression levels in LPS-stimulated and LPS-unstimulated prostate cancer cells. In conclusion, 6-Gingerol may induce protective autophagy, autophagic cell death and ferroptosis-mediated cell death in prostate cancer cells. These findings may provide a strategy for the treatment and prevention of prostate cancer.

## Introduction

Prostate cancer is a slowly developing disease with a high mortality rate in men, especially in Western countries (1). Castrate-resistant prostate cancer (CRPC) is resistant to androgen ablation and cancer metastases are often observed in patients with CRPC (2). Cancer metastasis is a complex mechanism and cascade of events that allows tumor cells to travel to other organs. Epithelial-mesenchymal transition (EMT) is as an important event in the initial steps of cancer cell metastasis (3). The loss of epithelial cell characteristics leads to the transformation of epithelial cells to mesenchymal cells with a stem cell-like phenotype. Notably, EMT can result in increasing resistance to apoptosis and chemotherapy (4,5). Previous studies have reported that lipopolysaccharide (LPS), a component of gram-negative bacteria, can trigger EMT, which induces the migration and invasion of cancer cells (6-8).

Autophagy regulates cell damage and degradation and processes the recycling of cell constituents. It is an adaptive process and a form of cell death that occurs in response to stress, including elevated levels of reactive oxygen species (ROS) and anticancer agents (9,10). Autophagy may therefore serve a pivotal role during chemotherapy. Phytochemicals or chemotherapeutic agents can overcome drug resistance and induce apoptosis in cancer cells (11-13).

Ferroptosis is a form of cell death, which has characteristics that are different from apoptosis and autophagy. The accumulation of intracellular iron and ROS, and the depletion of glutathione (GSH) are characteristic of ferroptosis (14).

*Correspondence to:* Dr Chi-Ming Liu, School of Medicine, Yichun University, 576 XueFu Road, Yuanzhou, Yichun, Jiangxi 336000, P.R. China  
E-mail: beagleliu@gmail.com

\*Contributed equally

**Key words:** 6-gingerol, epithelial-mesenchymal transition, ferroptosis, autophagy, prostate cancer

Ferroptosis inducers can inhibit cancer cell proliferation and may be a novel target for potential cancer therapeutics (15,16).

Dietary natural products contain numerous bioactive phytochemicals with a wide spectrum of pharmacological activities. Ginger (*Zingiber officinale*) is commonly used as a spice and a traditional medicine (17). One component of ginger extract, 6-Gingerol, has anti-inflammatory, anticancer and antioxidant effects (18-21). In addition, 6-Gingerol has been reported to exhibit synergistic effects on PC3 cells by inducing apoptosis (22) and to inhibit testosterone-induced proliferation of LNCaP cells (23). However, to the best of our knowledge, whether 6-Gingerol also inhibits EMT, and induces autophagy or ferroptosis in prostate cancer cells is unknown.

The present study aimed to determine the pharmacological effects of 6-Gingerol against LPS-induced migration and invasion, and the potential of 6-Gingerol to inhibit LPS-induced EMT in prostate cancer cells. It can therefore be hypothesized that 6-Gingerol may be used as an effective chemotherapeutic agent to treat prostate cancer.

## Materials and methods

**Chemicals and reagents.** 6-Gingerol (95-99% purity, determined by high-performance liquid chromatography) was purchased from Chengdu Biopurify Phytochemicals, Ltd. PI3K inhibitor (LY294002) and MTT reagent were purchased from Beyotime Institute of Biotechnology. LPS (from *Escherichia coli* 026:B6) and β-actin primary antibodies (cat. no. A5441) were obtained from MilliporeSigma. Ferrostatin-1 was purchased from Shanghai Aladdin Biochemical Technology Co., Ltd. Primary antibodies against Beclin-1 (cat. no. AB3219), LC3B (cat. no. CY5992), nuclear factor erythroid 2-related factor 2 (NRF2; cat. no. CY1851) and GSH peroxidase (GPX) 4 (cat. no. CY6959) were purchased from Shanghai Abways Biotechnology Co., Ltd. Primary antibodies against E-cadherin (cat. no. 3195), N-cadherin (cat. no. 13116), Vimentin (cat. no. 5741) and zonula occludens-1 (ZO-1; cat. no. 8193) were purchased from Cell Signaling Technology, Inc. Anti-rabbit IgG horseradish peroxidase HRP-linked antibody (cat. no. 7074) and anti-mouse IgG HRP-linked antibody (cat. no. 7076) were purchased from Cell Signaling Technology, Inc.

**Cell culture.** The human prostate cancer LNCaP, DU145 and PC3 cell lines were purchased from Shanghai Fuheng Biotechnology Co., Ltd. Cells were cultured at 37°C in a humidified atmosphere with 5% CO<sub>2</sub>. LNCaP cells were grown in RPMI-1640 medium, DU145 and PC3 cells were grown in DMEM/Ham's F12 Kaighn's (K) medium (both LONSERA ShangHai ShuangRu Biotech Co., Ltd). The media were supplemented with 10% fetal bovine serum (FBS; LONSERA ShangHai ShuangRu Biotech Co., Ltd.), 100 U/ml penicillin and 100 µg/ml streptomycin (Beyotime Institute of Biotechnology). In each experiment, the control group was untreated cells.

**Cell viability assay.** LNCaP, DU145 and PC3 cells were seeded at a density of 1x10<sup>4</sup> cells/well in 96-well plates. When cells reached 80% confluence, cells were treated with 6-Gingerol (1-500 µM), with or without LPS (1 µg/ml), ferrostatin-1

(5 µM) and LY294002 (10 µM), at 37°C for 24, 48 or 72 h. After incubation, cell viability was determined using an MTT assay. The medium was replaced with fresh medium, 10 µl MTT (5 mg/ml) was added to each well contain 100 µl fresh medium and cells were incubated at 37°C for 4 h. The supernatant was subsequently discarded and 100 µl DMSO was used to dissolve the MTT-formazan crystals. Absorbance was then quantified using a microplate reader at a wavelength of 570 nm.

**Colony formation.** LNCaP, DU145 and PC3 cells were seeded into a 6-well plate at a density of 5x10<sup>2</sup> cells/well. Cells were incubated at 37°C for 4 h and were subsequently treated with different concentrations (1, 10, 100 and 500 µM) of 6-Gingerol. After incubation at 37°C for 7 days without changing the medium, 4% formaldehyde was applied for fixing cells for 20 min at room temperature and stained with 0.2% crystal violet for 20 min at room temperature. Colonies were defined as groups of >50 cells and manually counted under an inverted light microscope (Nikon TI-DH).

**Wound healing assay.** DU145 and PC3 cells at a density of 1x10<sup>6</sup> cells/well were cultured on a 6-well plate with medium containing 10% FBS. After reaching 100% confluence, the medium was replaced with serum-free medium. A scratch was created on the cell monolayers using a sterile 200-µl pipette tip and cells were then treated with 6-Gingerol (10 µM), with or without LPS (1 µg/ml) at 37°C for 24 or 48 h. The images were observed and captured by image device (NIS Elements version 4.30, Nikon) and inverted light microscope (Nikon TI-DH). Wound healing was semi-quantified using ImageJ 1.52a software (National Institutes of Health). The wound area was calculated as the follows: (Initial wound width-final wound width)/initial wound width x100 (%).

**Cell adhesion assay.** Fibronectin (Beijing Solarbio Science & Technology Co., Ltd.) was dissolved in PBS and used for coating. Then, 0.1 ml of fibronectin (5 µg/ml) was added per well in a 96-well plate at 4°C overnight. After incubation, the wells were washed with PBS twice and incubated with serum-free medium at 37°C for 30 min. LNCaP, DU145 and PC3 cells (1x10<sup>4</sup>) were added to each well in fresh medium containing 6-Gingerol (100 and 500 µM), with or without LPS (1 µg/ml) incubated at 37°C at 1 and 2 h for adhesion. After incubation, the adhered cells were gently washed twice with PBS and measured using MTT assay, as aforementioned.

**Migration and invasion assays.** The migratory and invasive abilities of DU145 and PC3 cells were determined using 8-µm Transwell filter membranes (Costar; Corning, Inc.). For the migration assay, 1x10<sup>4</sup> cells were seeded into the upper chamber with DMEM/Ham's F12K serum-free medium containing 6-Gingerol (10 µM), whereas the bottom chamber was loaded with DMEM/Ham's F12K medium containing 10% FBS with or without LPS (1 µg/ml) as a chemoattractant. After incubation at 37°C for 48 h, cells in the upper chamber were gently scraped off and the migrating cells that had accumulated in the bottom chamber were fixed with 4% formaldehyde for 20 min at room temperature and stained with 0.2% crystal violet for 20 min at room temperature. The migrated cells on the

bottom surface of the membrane were captured (NIS Elements version 4.30, Nikon) and counted manually under an inverted light microscope (Nikon TI-DH). For the invasion assay, each Transwell plate was coated with Matrigel (1 mg/ml, Corning, Inc.) with serum free medium at 37°C for 1 h. The subsequent procedure was the same as that of migration assay.

**Western blotting.** To examine the mechanism of underling the anti-cancer effects of 6-Gingerol on prostate cancer cells, LNCaP, DU145 and PC3 cells were treated with 6-Gingerol (1-100  $\mu$ M), with or without LPS (1  $\mu$ g/ml) and ferrostatin-1 (5  $\mu$ M) at 37°C for 24 or 48 h. After incubation, total protein was extracted by M-PER mammalian protein extraction reagent (Thermo Fisher Scientific, Inc.; cat. no. 78505). The concentration of protein was determined by Pierce Coomassie (Bradford) Protein Assay Kit (Thermo Scientific, cat. no. 23200) and was separated by 7.5, 10.0 or 12.0% SDS-PAGE (20  $\mu$ g total protein/lane). Separated proteins were subsequently transferred onto a PVDF membrane. The membranes were blocked with 5% non-fat dried milk 1X TBST buffer (20 mM Tris, 150 mM NaCl, 0.1% Tween 20) at room temperature for 1 h. Membranes were incubated at 4°C overnight with the following primary antibodies: Beclin-1 (1:1,000), LC3B (1:1,000), NRF2 (1:1,000), GPX4 (1:1,000), E-cadherin (1:1,000), N-cadherin (1:1,000), Vimentin (1:1,000),  $\beta$ -actin (1:8,000) and ZO-1 (1:1,000). Subsequently, membranes were incubated for 1 h at room temperature with the secondary antibodies, anti-rabbit IgG HRP-linked antibody (1:1,000) and anti-mouse IgG HRP-linked antibody (1:1,000). Protein bands were subsequently visualized using an enhanced chemiluminescent kit to determine protein expression (Shanghai Epizyme Biomedical Technology Co., Ltd). The bands were detected using a ChemiScope 3300 Mini (Clinx Science Instruments Co., Ltd.).  $\beta$ -actin was used as the internal control for Western Blots. The densitometry of protein expression was determined using ImageJ 1.52a software (National Institutes of Health, USA).

**Determination of intracellular ROS and GSH.** Intracellular ROS levels were determined using reactive oxygen species assay kit (Biosharp; cat. no. BL714A), according to the manufacturer's protocol. Briefly, the LNCaP, DU145 and PC3 cells were cultured in 6-well plates at density of 1 $\times$ 10<sup>5</sup> cells. Cells were treated with 6-Gingerol (100  $\mu$ M) with or without ferrostatin-1 (5  $\mu$ M) at 37°C for 24 h. After the incubation, the cells were collected, stained with H2DCFH-DA (10  $\mu$ M) at 37°C for 30 min in the dark and then washed twice with serum free medium. For each experiment, the fluorescence intensity of ROS was quantified using flow cytometry (NovoCyte Flow Cytometer; Agilent Technologies, Inc.). Data were analyzed using NovoExpress 1.2.5 software (2016 ACEA Biosciences, Inc.). GSH levels were determined using a Glutathione Assay Kit (Nanjing Jiancheng Bioengineering Institute; cat. no. A006-2-1). LNCaP, DU145 and PC3 cells at the density of 1 $\times$ 10<sup>4</sup> were seeded into a 24-well plate and incubated overnight at 37°C. Cells were treated with 6-Gingerol (10, 100  $\mu$ M) with or without ferrostatin-1 (5  $\mu$ M) at 37°C for 24 h. Cells were then collected and homogenized. After centrifugation at 14,000 g for 10 min at 4°C, the supernatant was collected and GSH levels quantified according to the manufacturer's

instructions. The absorbance was measured using a microplate reader at the wavelength of 405 nm. The content of GSH levels were determined by the standard curve.

**Statistical analysis.** The experiments were performed at three times independently and the data analysis were done by Excel (Microsoft 365MSO, 16.0.14931.20118). Statistical comparisons among more than two groups were performed using one-way ANOVA followed by Tukey's post hoc test. All data are presented as the mean  $\pm$  SEM. P<0.05 was considered to indicate a statistically significant difference.

## Results

**6-Gingerol suppresses cell viability and colony formation in prostate cancer cells.** LNCaP, PC3 and DU145 cells were treated with 6-Gingerol (1-500  $\mu$ M) for 24, 48 or 72 h. The viability of LNCaP, PC3 and DU145 cells was inhibited by the different 6-Gingerol (1-500  $\mu$ M) treatments. The cell survival rate with 6-Gingerol (500  $\mu$ M) at 72 h was 46.08 $\pm$ 4.29, 47.20 $\pm$ 5.90 and 50.59 $\pm$ 4.20% in LNCaP, PC3 and DU145 cells, respectively (Fig. 1A). Colony formation in the presence of 6-Gingerol was also investigated. The colony number determined for each treatment group (1-500  $\mu$ M, 6-Gingerol) was significantly reduced compared with the control group in LNCaP, PC3 and DU145 cells (Figs. 1B and S1), which suggested that 6-Gingerol inhibited cell viability and colony formation in prostate cancer cells. Furthermore, the cell survival rate of LNCaP, PC3 and DU145 cells treated with LPS was assessed (Fig. 1C). Several studies reported that LPS can enhance the metastasis and invasion in prostate and breast cancer cells (6-8). LPS (1  $\mu$ g/ml) was not cytotoxic to any of the cell lines; this concentration was therefore selected to assess the adhesion, invasion, migration and EMT effects on prostate cancer cells. 6-Gingerol (100  $\mu$ M) can significantly inhibit LPS-induced cell growth at 48 and 72 h (Fig. 1C). Overall, these results indicated that 6-Gingerol may exhibit cytotoxicity in a dose-dependent manner in LNCaP, PC3 and DU145 cells.

**6-Gingerol attenuates migration, invasion and adhesion in prostate cancer cells.** CRPC is an aggressive disease, and it is not sensitive to medical castration with higher potential of invasion and metastasis (2). PC3 and DU145 cells are CRPC cells (7). Therefore, we selected PC3 and DU145 cells for migration and invasion assay. To investigate the mechanism of 6-Gingerol in cell migration and invasion, the wound healing and Transwell assays were performed. The results demonstrated that cell migration and invasion were significantly enhanced in LPS-induced DU145 cells. However, only cell invasion was significantly enhanced in LPS-induced PC3 cells (Figs. 2 and 3). Moreover, 6-Gingerol (10  $\mu$ M) significantly inhibited migration and invasion in LPS-treated or LPS-untreated PC3 and DU145 cells at 48 h, compared with the LPS or control groups, respectively.

Cell attachment to the extracellular matrix is important for cell metastasis in distant organs (24); therefore, the effect of 6-Gingerol on prostate cancer cell adhesion to extracellular matrix proteins was investigated. Fibronectin (5  $\mu$ g/ml) significantly induced adhesion in DU145 and LNCaP cells at 2 h

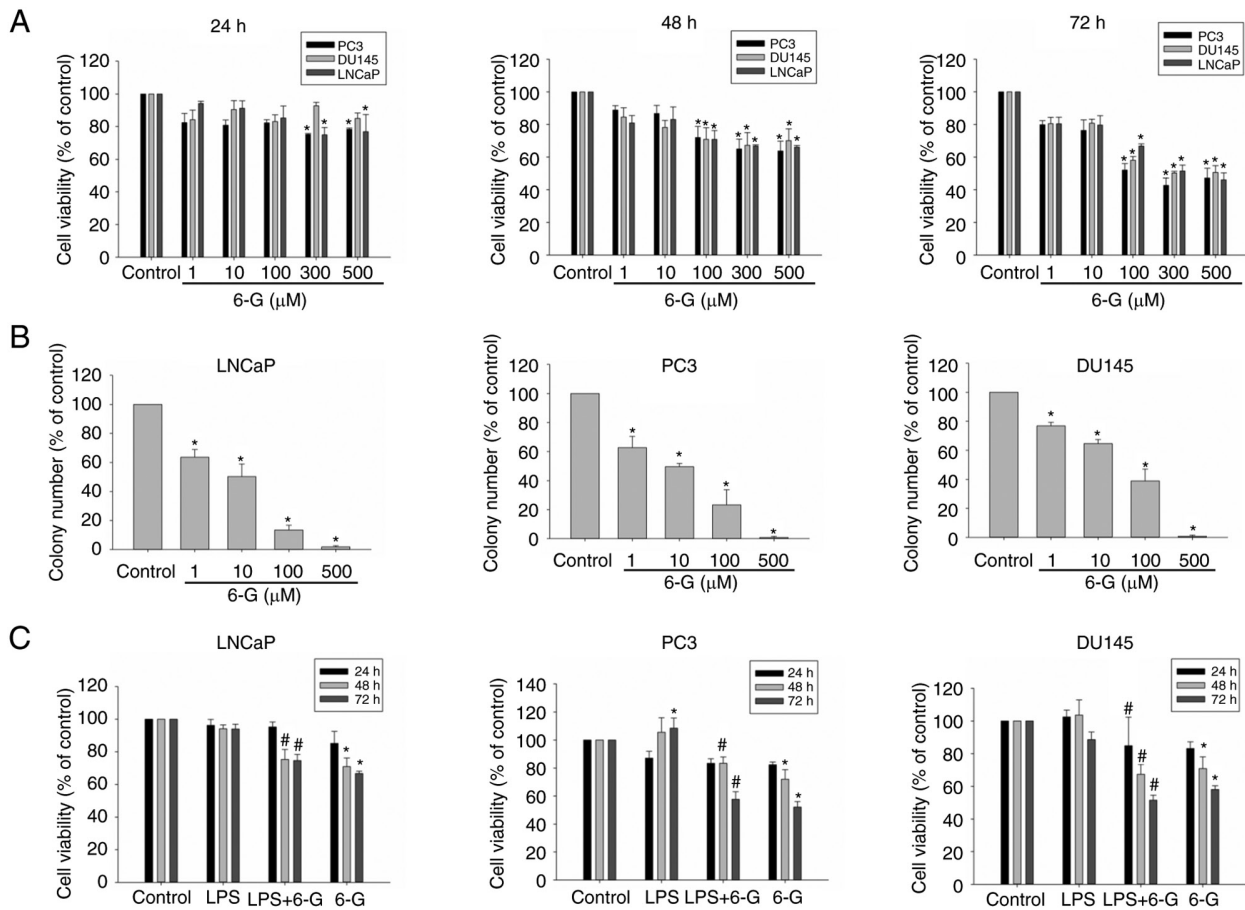


Figure 1. 6-G suppresses prostate cancer cell viability. (A) Viability of LNCaP, PC3 and DU145 cells incubated with 6-G. (B) Colony formation of LNCaP, PC3 and DU145 cells incubated with 6-G for 7 days. (C) Cell viability following treatment with 6-G (100  $\mu$ M) with or without LPS (1  $\mu$ g/ml). Data are presented as the mean  $\pm$  SEM from three independent experiments. \*P<0.05 vs. control; #P<0.05 vs. LPS. 6-G, 6-Gingerol; LPS, lipopolysaccharide.

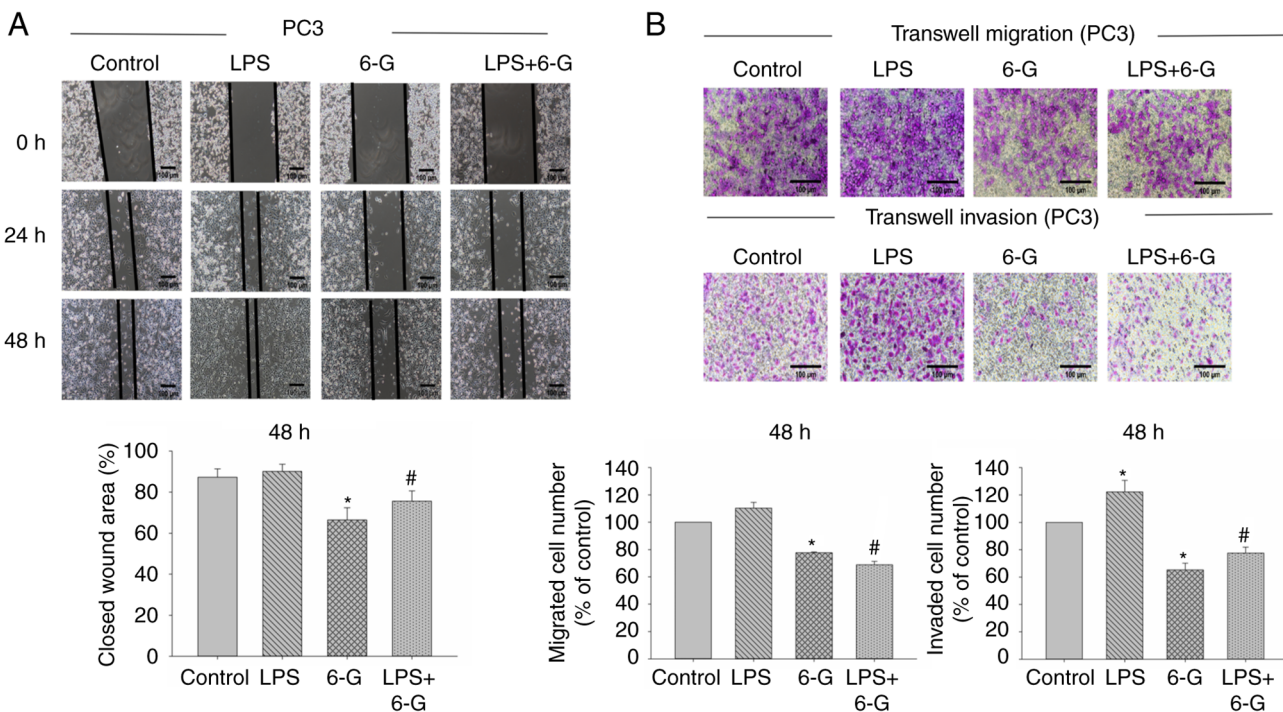


Figure 2. 6-G inhibits migration and invasion of LPS-stimulated and LPS-unstimulated PC3 cells. The anti-migratory and anti-invasive effects of 6-G (10  $\mu$ M) with or without LPS (1  $\mu$ g/ml) on PC3 cells were determined using (A) wound healing (magnification,  $\times 100$ ) and (B) Transwell assays (magnification,  $\times 200$ ). Scale bar=100  $\mu$ m. Data are presented as the mean  $\pm$  SEM from three independent experiments. \*P<0.05 vs. control; #P<0.05 vs. LPS. 6-G, 6-Gingerol; LPS, lipopolysaccharide.

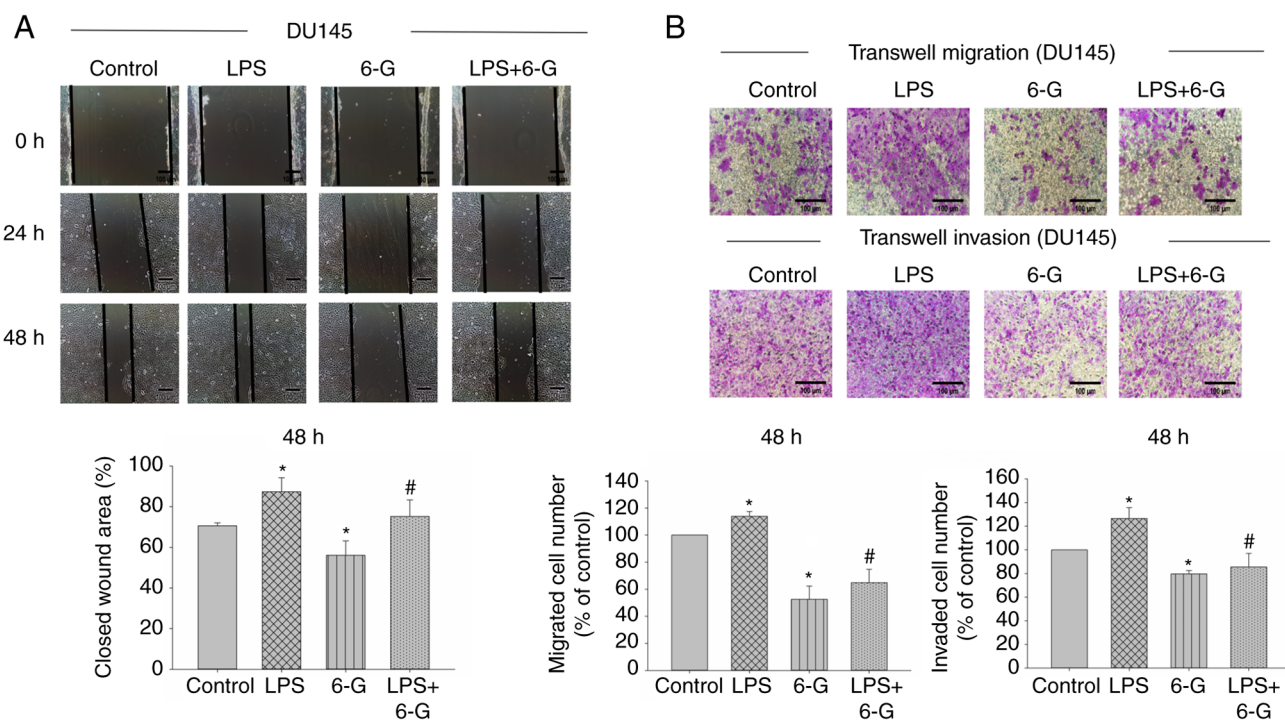


Figure 3. 6-G inhibits migration and invasion of LPS-stimulated and LPS-unstimulated DU145 cells. The anti-migration and anti-invasion effects of 6-G ( $10 \mu\text{M}$ ) with or without LPS ( $1 \mu\text{g/ml}$ ) on DU145 cells were determined using (A) wound healing (magnification,  $\times 100$ ) and (B) Transwell migration assays (magnification,  $\times 200$ ). Scale bar= $100 \mu\text{m}$ . Data are presented as the mean  $\pm$  SEM of three independent experiments. \* $P<0.05$  vs. control; # $P<0.05$  vs. LPS. 6-G, 6-Gingerol; LPS, lipopolysaccharide.

(Fig. 4A). 6-Gingerol ( $100$  and  $500 \mu\text{M}$ ) significantly inhibited fibronectin-treated attachment at  $2 \text{ h}$  in LNCaP, DU145 and PC3 cells (Fig. 4A). The results demonstrated that LPS significantly enhanced the binding affinity of PC3, DU145 and LNCaP cells to fibronectin compared with the group treated with LPS alone at  $2 \text{ h}$  (Fig. 4B). 6-Gingerol ( $100$ ,  $500 \mu\text{M}$ ) significantly decreased the binding affinity of LNCaP, PC3 and DU145 cells to fibronectin with or without LPS treatment compared with the LPS + fibronectin or fibronectin group, respectively at  $2 \text{ h}$  (Fig. 4). These results indicated that 6-Gingerol may have anti-invasion, anti-migration and anti-adhesion properties in prostate cancer cells.

**6-Gingerol induces autophagy in prostate cancer cells.** Subsequently it was determined if 6-Gingerol could induce autophagy in prostate cancer cells using western blotting to analyze Beclin-1 and LC3B protein expression levels. LC3B-II is important in autophagy and can be used as an autophagy marker (25). The results demonstrated that 6-Gingerol ( $10$ - $100 \mu\text{M}$ ) significantly induced LC3B-II protein expression levels in LNCaP cancer cells compared with the control (Fig. 5A). The LC3B-II protein expression levels were significantly upregulated in 6-Gingerol-treated ( $1$ - $10 \mu\text{M}$ ) PC3 cells. However, this was not observed in DU145 cells, due to the absence of the ATG5 protein, which results in ATG12/ATG5 conjugate deficiency (26). 6-Gingerol ( $10$ - $100 \mu\text{M}$ ) significantly upregulated Beclin-1 protein expression levels in LNCaP, PC3 and DU145 cells compared with the control (Fig. 5A). LY294002, a known PI3K and autophagy inhibitor, slightly enhanced 6-Gingerol cytotoxicity in LNCaP and PC3 cells (Fig. S2); however, this effect was significantly reversed

in DU145 cells compared with the 6-Gingerol group (Fig. 5B). These results therefore indicated that 6-Gingerol potentially induced protective autophagy in LNCaP and PC3 cells but promoted autophagic cell death in DU145 cells. The results suggested that 6-Gingerol induced autophagy by regulating LC3B-II and Beclin-1 protein expression levels in LNCaP and PC3 cells. Moreover, 6-Gingerol also induced autophagy by inducing Beclin-1 and LC3B-I but without LC3B-II protein expression in DU145 cells.

**6-Gingerol suppresses EMT-related protein expression in prostate cancer cells.** EMT serves a significant role in cancer progression and metastasis, a mechanism which LPS can trigger and enhance (6-8). The protein expression levels of E-cadherin, N-cadherin, Vimentin and ZO-1 were examined following 6-Gingerol ( $1$ - $100 \mu\text{M}$ ) treatment for  $24 \text{ h}$  in LNCaP, PC3 and DU145 cells. The results demonstrated that E-cadherin and ZO-1 were significantly upregulated in 6-Gingerol-treated ( $10$ - $100 \mu\text{M}$ ) prostate cancer cells compared with the control (Fig. 6); however, N-cadherin and Vimentin were downregulated in 6-Gingerol-treated PC3 and LNCaP cells. The protein expressions of N-cadherin were not significantly inhibited by 6-Gingerol ( $1$ - $100 \mu\text{M}$ ) treatment for  $24 \text{ h}$  in DU145 cells. Cell invasion and migration were significantly induced after LPS treatment in DU145 cells. Therefore, DU145 cells were selected for examining the underlying mechanism of action of EMT in LPS-treated DU145 cells. Furthermore, the results indicated that LPS significantly induced N-cadherin and Vimentin protein expression levels in DU145 cells at  $48 \text{ h}$  compared with the control (Fig. 7A and C). In addition, 6-Gingerol did not markedly increased E-cadherin

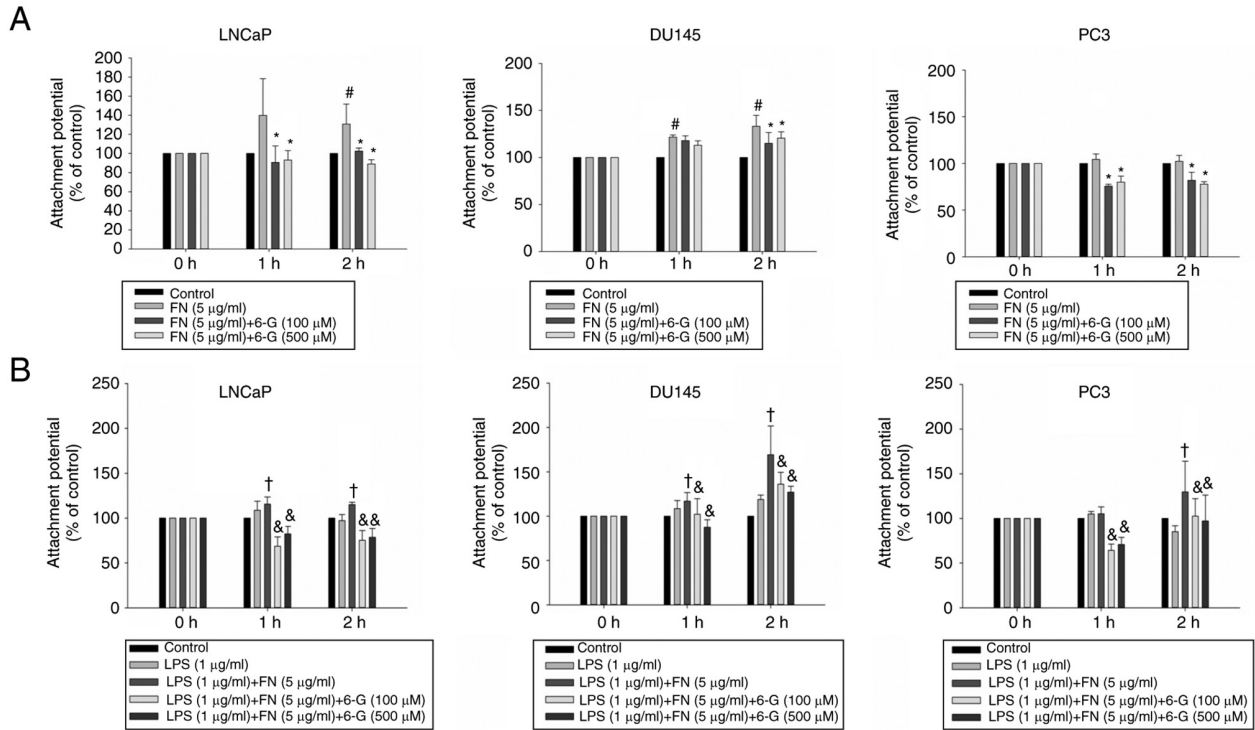


Figure 4. Effect of 6-G on LNCaP, PC3 and DU145 prostate cancer cell attachment on FN (5  $\mu$ g/ml)-coated plates. (A) LPS-unstimulated and (B) LPS-stimulated prostate cancer cells were treated with 6-G (100 or 500  $\mu$ M). Attached cells were determined using an MTT assay. \*P<0.05 vs. FN; #P<0.05 vs. control; &P<0.05 vs. LPS + FN; †P<0.05 vs. LPS. 6-G, 6-Gingerol; FN, fibronectin; LPS, lipopolysaccharide.

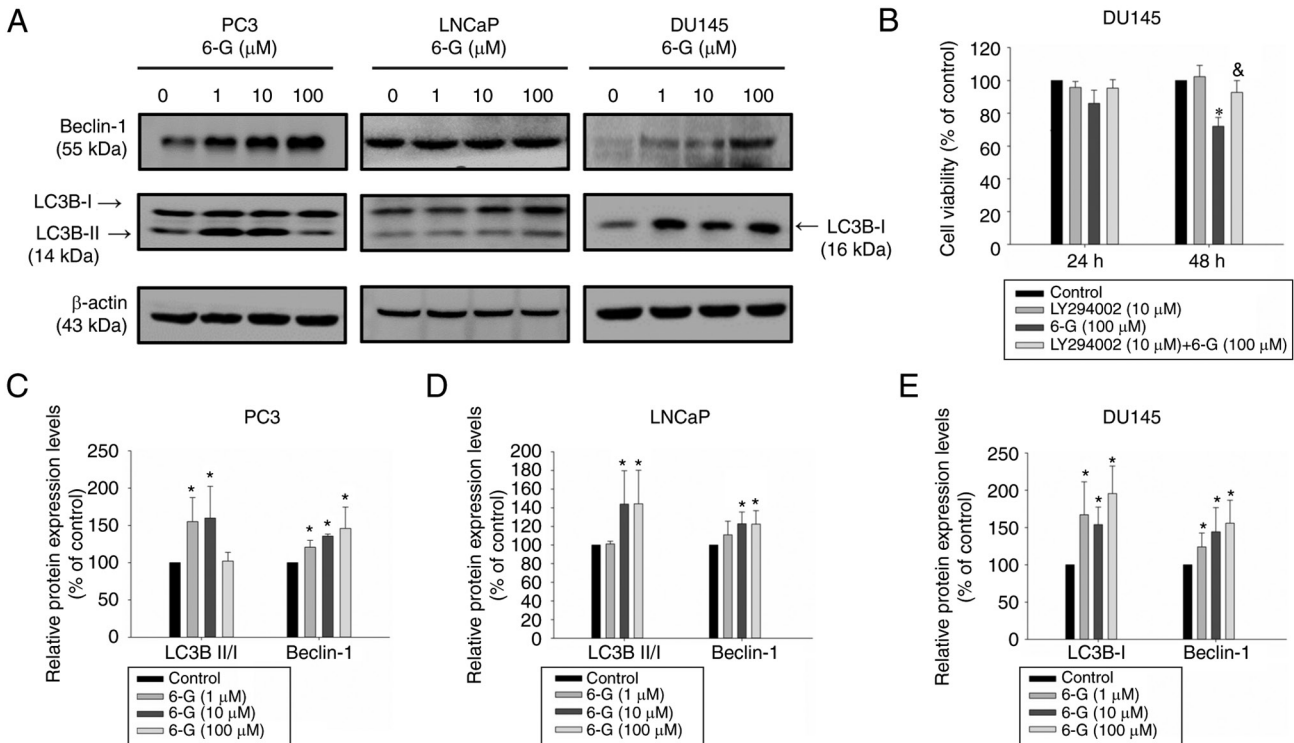


Figure 5. 6-G induces autophagy in prostate cancer cells. (A) Prostate cancer cells were treated with 6-G (1–100  $\mu$ M) for 24 h. The protein expression levels of Beclin-1 and LC3B were determined via western blotting. (B) 6-Gingerol-treated cell viability in the presence or absence of LY294002 (10  $\mu$ M) in DU145 cells incubated for 24 and 48 h. Semi-quantification of Beclin-1 and LC3B protein expression levels were performed using image analysis in (C) PC3, (D) LNCaP and (E) DU145 cells. \*P<0.05 vs. control; &P<0.05 vs. 6-G (100  $\mu$ M). 6-G, 6-Gingerol.

protein expression levels, whereas it significantly downregulated N-cadherin and Vimentin protein expression levels in the

LPS + 6-Gingerol group compared with the LPS group. The results also demonstrated that the protein expression levels of

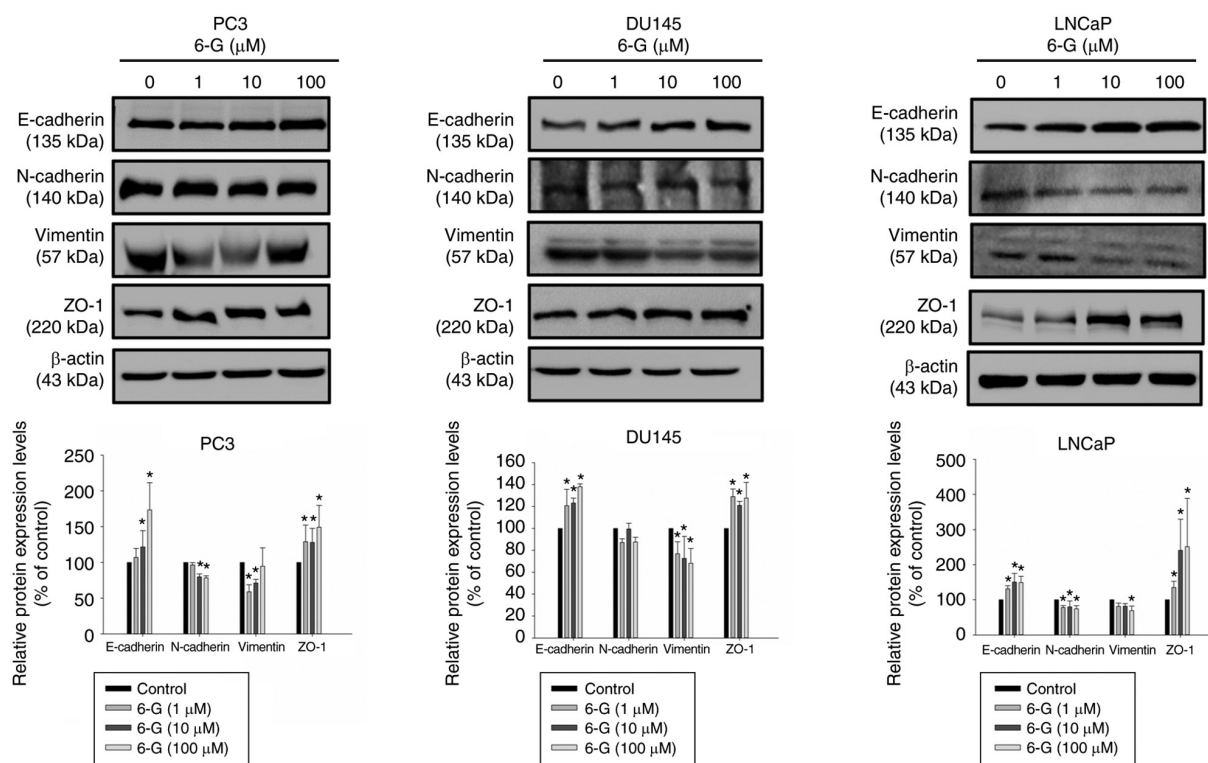


Figure 6. 6-G inhibits the epithelial-mesenchymal transition in prostate cancer cells. Prostate cancer cells were treated with 6-G (1–100 μM) for 24 h. The protein expression levels of E-cadherin, N-cadherin, Vimentin and ZO-1 were analyzed via western blotting. \*P<0.05 vs. control. 6-G, 6-Gingerol; ZO-1, zonula occludens-1.

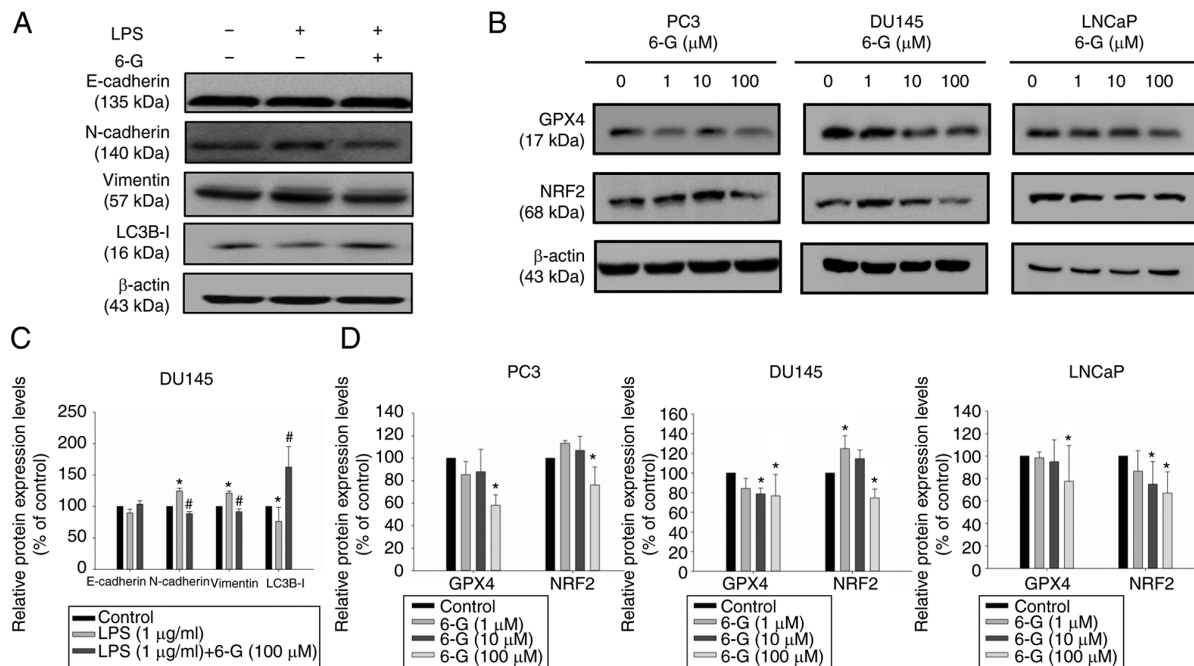


Figure 7. Effects of 6-G treatment on autophagy, the epithelial-mesenchymal transition and ferroptosis in LPS-stimulated and LPS-unstimulated prostate cancer cells. (A) DU145 cells were treated with 6-G (100 μM) with or without LPS (1 μg/ml) for 48 h. Western blotting was performed to determine the protein expression levels of E-cadherin, N-cadherin, Vimentin and LC3B-I. (B) NRF2 and GPX4 protein expression levels following 6-G treatment for 24 h were determined via western blotting. (C) Semi-quantification of E-cadherin, N-cadherin, Vimentin and LC3B-I protein expression levels was performed using image analysis. (D) Semi-quantification of GPX4 and NRF2 protein expression levels was performed using image analysis. \*P<0.05 vs. control; #P<0.05 vs. LPS. 6-G, 6-Gingerol; LPS, lipopolysaccharide; GPX4, glutathione peroxidase 4; NRF2, nuclear factor erythroid 2-related factor 2.

LC3B-I were significantly decreased in LPS-stimulated DU145 cells compared with the control. 6-Gingerol (100 μM) reversed

the protein expression levels of LC3B-I in LPS-stimulated DU145 cells. These data indicated that LPS potentially

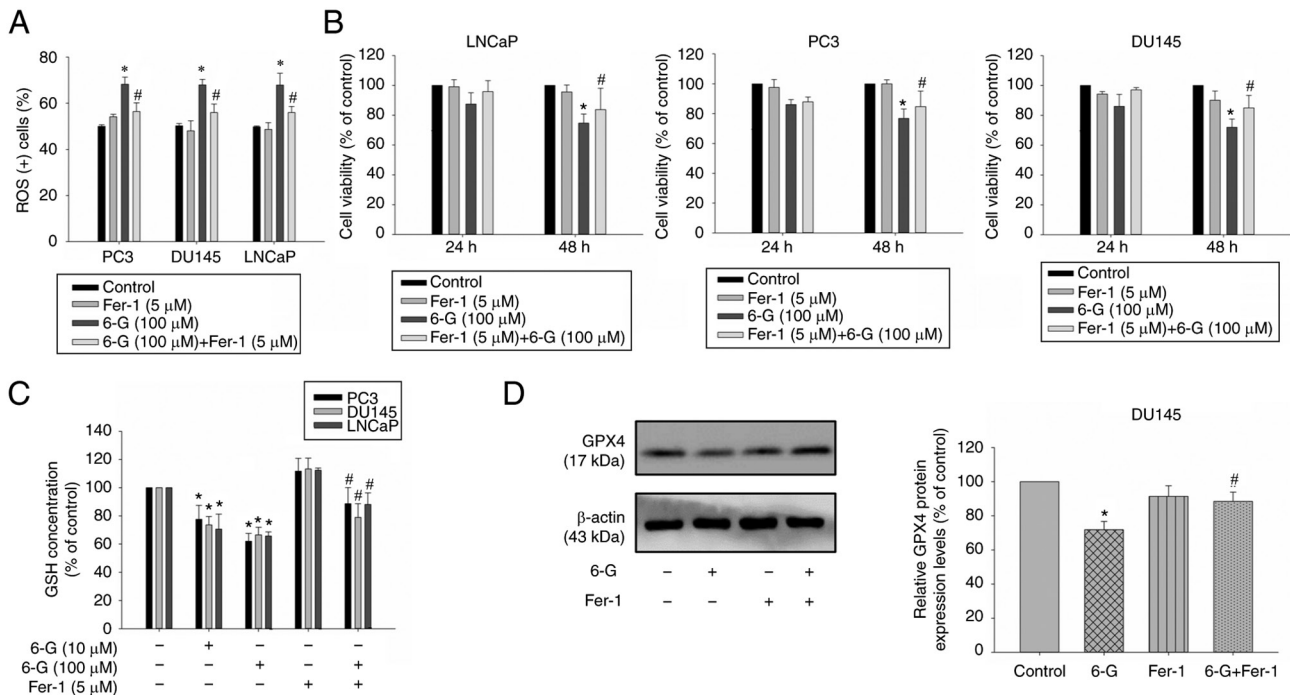


Figure 8. 6-G triggers ferroptosis in LNCaP, PC3 and DU145 cells. (A) ROS levels in prostate cancer cells following 6-G treatment with or without Fer-1 (5  $\mu$ M) for 24 h. (B) Cytotoxicity of 6-G (100  $\mu$ M) with or without Fer-1 (5  $\mu$ M) for 24 and 48 h in prostate cancer cells. (C) GSH concentration in prostate cancer cells following 6-G treatment with or without Fer-1 (5  $\mu$ M) for 24 h. (D) GPX4 protein expression levels following 6-G (100  $\mu$ M) treatments with or without Fer-1 (5  $\mu$ M) for 24 h in DU145 cells. \* $P$ <0.05 vs. control; # $P$ <0.05 vs. 6-G (100  $\mu$ M). 6-G, 6-Gingerol; ROS, reactive oxygen species; Fer-1, ferrostatin-1; GSH, glutathione.

stimulated EMT and that 6-Gingerol may reverse these effects on EMT in LPS-treated prostate cancer cells.

**6-Gingerol treatment induces ferroptosis.** Ferroptosis is associated with ROS production, which leads to decreased cellular GSH levels (27). GPX4 is an enzyme that belongs to the family of GPXs and GPX4 inactivation can promote ferroptosis (28). Therefore, the role of ROS, GSH, GPX4 and NRF2 protein expression in prostate cancer cells was determined. GPX4 and NRF2 protein expression levels were significantly down-regulated after 24 h of 6-Gingerol (100  $\mu$ M) treatment in LNCaP, PC3 and DU145 cells (Fig. 7B and D). NRF2 protein expression levels were increased after 6-Gingerol (1–10  $\mu$ M) treatment in PC3 and DU145 cells, but this was not observed in LNCaP cells. PC3 and DU145 are castration-resistant prostate cancer cells, and LNCaP is androgen-dependent prostate cancer cell line (18,29). This might slightly increase NRF2 levels after low concentration of 6-Gingerol treatment in PC3 and DU145 cells because of castration-resistant prostate cancer cells. Furthermore, ROS levels were significantly increased following 6-Gingerol treatment in LNCaP, PC3 and DU145 cells compared with the control. Notably, this effect was significantly attenuated by pre-treatment with ferrostatin-1, compared with the 6-Gingerol only group (Figs. 8A and S3).

To further determine the effect of 6-Gingerol on cell death, ferrostatin-1, an effective ferroptosis inhibitor, was used. The results demonstrated that ferrostatin-1 significantly alleviated a decrease in cell viability in LNCaP, PC3 and DU145 cells at 48 h in cells treated with 6-Gingerol (100  $\mu$ M) compared with the 6-Gingerol group (Fig. 8B). GSH levels were also

significantly reduced after 6-Gingerol treatment (10–100  $\mu$ M) compared with the control; however, this effect was significantly attenuated by pre-treatment with ferrostatin-1 (5  $\mu$ M) compared with the 6-Gingerol group (100  $\mu$ M) (Fig. 8C). GPX4 protein expression levels were attenuated following 6-Gingerol (100  $\mu$ M) treatment for 24 h in DU145 cell. The expression was significantly increased in ferrostatin-1 pre-treatment 6-Gingerol-treated (100  $\mu$ M) DU145 cells compared with the 6-Gingerol group (Fig. 8D). These results indicated that cell death may be mediated by a ferroptosis mechanism. Furthermore, these data indicated that 6-Gingerol may induce ROS accumulation and ferroptosis; therefore, ferroptosis may be a potential mechanism, induced by 6-Gingerol, against prostate cancer cell proliferation.

## Discussion

6-Gingerol has been reported to induce apoptosis in numerous types of cancer cells, including breast cancer, colon cancer, prostate cancer and cervical cancer cells (21,30–32). In addition, it may regulate both multidrug resistance-associated protein 1 and glutathione S-transferase in docetaxel-resistant prostate cancer cells (21). To the best of our knowledge, no study has focused on the anti-migratory and anti-invasive activity of 6-Gingerol in prostate cancer cells. In the present study, it was reported that 6-Gingerol affected human androgen-dependent (LNCaP) and castrate-resistant (DU145 and PC3) prostate cancer cells by inducing autophagy and ferroptosis. The results also demonstrated that 6-Gingerol significantly inhibited cell migration and invasion via the regulation of EMT-related proteins in prostate cancer cells.

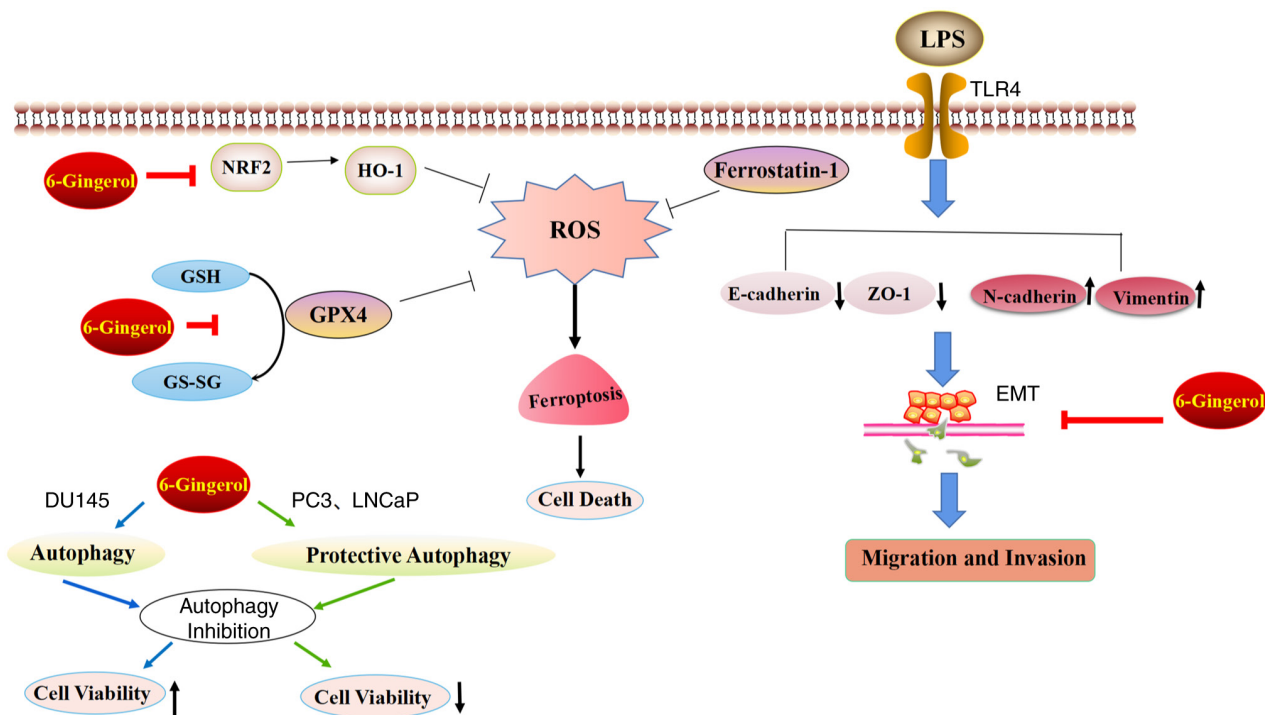


Figure 9. Diagram demonstrating the inhibition of cell proliferation and EMT in prostate cancer cells following 6-Gingerol treatment. In the present study, 6-Gingerol induced autophagy and ferroptosis. 6-Gingerol also reversed the EMT in LPS-treated and LPS-untreated prostate cancer cells. EMT, epithelial-mesenchymal transition; LPS, lipopolysaccharide; TLR4, toll-like receptor 4; NRF2, nuclear factor erythroid 2-related factor 2; GSH, glutathione; GPX4, glutathione peroxidase 4; ZO-1, zonula occludens-1; HO-1, heme oxygenase-1; GS-SG, oxidized glutathione.

EMT serves a significant role in cancer progression, whereby epithelial cells lose cell polarity and are transformed into cells with a mesenchymal phenotype, which exhibit increased migratory and invasive abilities in combination with reduced intracellular adhesion (33). EMT is also associated with cancer stem cell-like properties and chemotherapy drug resistance (4). Therefore, a therapeutic agent that can effectively inhibit the EMT process may be a potential anti-metastatic strategy. Cadherins, named for ‘calcium-dependent adhesion’, serve a key role in adherens junctions (34). A loss in E-cadherin expression can result in the loss of contact inhibition, and increase cell motility and invasion (35). Notably, N-cadherin is expressed in mesenchymal cells and is overexpressed in cancer cells (36). Vimentin is an intermediate filament protein, which is a cytoskeletal component in mesenchymal cells (37). In the present study, it was demonstrated that E-cadherin and ZO-1 protein expression levels were significantly upregulated following 6-Gingerol treatment in prostate cancer cells, whereas the mesenchymal markers, Vimentin and N-cadherin were significantly decreased following 6-Gingerol treatment in the PC3 and LNCaP cell lines. Our previous study reported that LPS can enhance cell migration, invasion and inflammation in prostate cancer cells (8). LPS is known to induce EMT in prostate and breast cancer cells, which results in metastasis (7,38). In the present study, the results demonstrated that LPS stimulated EMT progression by significantly increasing Vimentin and N-cadherin and did not markedly attenuate E-cadherin protein expression levels in DU145 cells. Cell invasion and migration were significantly induced following LPS treatment, whereas 6-Gingerol significantly suppressed cell migration and invasion, and EMT by reversing

this pattern of EMT protein expression levels in LPS-treated DU145 cells.

Autophagy is a form of cell death that can remove mis-folded proteins and maintain cellular homeostasis under stressful conditions; notably, excess autophagy can also result in cell death (39). Therefore, the induction or inhibition of autophagy is considered to be a potential novel strategy for the treatment of cancer (39). In the present study, 6-Gingerol significantly induced LC3B conversion and Beclin-1 protein expression in prostate cancer cells. However, autophagy inhibitor LY294002 increased 6-Gingerol-induced cell death in PC3 and LNCaP cells. Previous studies have reported that autophagy serves a cytoprotective role against apoptosis (39,40). These results revealed that autophagy induction of 6-Gingerol might protect PC3 and LNCaP cells from cytotoxicity effects. However, cell viability was increased following 6-Gingerol combined with LY294002 treatment in DU145 cells. Protective autophagy (PC3 and LNCaP) and autophagic cell death (DU145) were observed after 6-Gingerol treatment in prostate cancer cells.

Recent studies have demonstrated that ferroptosis is important in the regulation of tumor cell proliferation, including in breast, lung and prostate cancer (41–43). Therefore, ferroptosis may be a potential novel strategy and therapeutic target for the treatment of cancer. Ferroptosis results from the depletion of GSH, GPX4 inactivation and intracellular ROS accumulation (44). In the present study, 6-Gingerol significantly decreased the levels of GPX4 and GSH, and significantly elevated ROS accumulation in PC3, DU145 and LNCaP cells. Previous studies have reported that 6-Gingerol-induced ROS production is accompanied by apoptosis in gastric cancer, human epidermoid carcinoma and myeloid leukemia cells (45–47).

The results of the present study demonstrated that 6-Gingerol may have significantly induced ROS production via a ferroptosis mechanism in prostate cancer cells and that pretreatment with the ferroptosis inhibitor, ferrostatin-1, significantly reversed 6-Gingerol-induced ferroptosis. NRF2 is a transcription factor that regulates signaling pathways in response to oxidative stress. Inhibition or knockdown of the NRF2 gene has been shown to enhance ferroptosis that results in decreased GSH synthesis and GPX4 inhibition (48,49). The present study demonstrated that 6-Gingerol (100  $\mu$ M) significantly decreased NRF2 protein expression levels in prostate cancer cells. Taken together, these data suggested that 6-Gingerol may promote ferroptosis, which could be beneficial for the treatment of prostate cancer. Furthermore, these results indicated that ferroptosis potentially serves an important role in mediating cell death in DU145 cells treated with 6-Gingerol.

6-Gingerol is a flavonoid antioxidant that is enriched in fresh ginger. Numerous studies have reported that 6-Gingerol has anticancer and anti-inflammatory effects (20,50-53). The present study provided new evidence that 6-Gingerol may have potential anti-metastatic and anticancer activities in prostate cancer cells (Fig. 9). 6-Gingerol significantly regulated EMT-related protein expression levels in LPS-stimulated and LPS-unstimulated prostate cancer cells. Furthermore, 6-Gingerol may trigger autophagy and ferroptosis, which suggested that both mechanisms may serve pivotal roles in regulating cell survival. In summary, 6-Gingerol may be considered an important novel therapeutic agent for the prevention and treatment of prostate cancer as a result of its numerous pharmacological activities. Our study demonstrated that 6-Gingerol can suppress migration, invasion and cell survival in CRPC, and androgen-dependent prostate cancer cells. *In vivo* studies are needed to verify these results in the future.

## Acknowledgements

Not applicable.

## Funding

The present study was supported by the Yichun University Local Development Research Center (grant no. DF2019002) and the PhD Research Foundation of Yichun University (grant no. 211-3360118006).

## Availability of data and materials

The datasets used and/or analyzed during the current study are available from the corresponding author on reasonable request.

## Authors' contributions

CML and LA designed the present study and performed the experiments. MS, ZS, YL and XL helped to perform the experiments. CML, ZW, AJO and YJ contributed to the conception of the study and analyzed the data. CML and LA confirm the authenticity of all the raw data. CML and LA wrote the manuscript. CML approved the version to be published and provided funding. All authors read and approved the final version of the manuscript.

## Ethics approval and consent to participate

Not applicable.

## Patient consent for publication

Not applicable.

## Competing interests

The authors declare that they have no competing interests.

## References

- Schatten H: Brief overview of prostate cancer statistics, grading, diagnosis and treatment strategies. *Adv Exp Med Biol* 1095: 1-14, 2018.
- Logothetis C, Morris MJ, Den R and Coleman RE: Current perspectives on bone metastases in castrate-resistant prostate cancer. *Cancer Metastasis Rev* 37: 189-196, 2018.
- Suarez-Carmona M, Lesage J, Cataldo D and Gilles C: EMT and inflammation: Inseparable actors of cancer progression. *Mol Oncol* 11: 805-823, 2017.
- Du B and Shim JS: Targeting epithelial-mesenchymal transition (EMT) to overcome drug resistance in cancer. *Molecules* 21: 965, 2016.
- Saitoh M: Involvement of partial EMT in cancer progression. *J Biochem* 164: 257-264, 2018.
- Huang T, Chen Z and Fang L: Curcumin inhibits LPS-induced EMT through downregulation of NF- $\kappa$ B-snail signaling in breast cancer cells. *Oncol Rep* 29: 117-124, 2013.
- Tian QX, Zhang ZH, Ye QL, Xu S, Hong Q, Xing WY, Chen L, Yu DX, Xu DX and Xie DD: Melatonin inhibits migration and invasion in LPS-stimulated and -unstimulated prostate cancer cells through blocking multiple EMT-relative pathways. *J Inflamm Res* 14: 2253-2265, 2021.
- Wu Z, Chen CY, Kao CL, Jiang Y and Liu CM: Docosahexaenoic acid inhibits lipopolysaccharide-induced metastatic activities by decreasing inflammation on prostate cancer cell. *Pharmazie* 74: 675-679, 2019.
- Li X, He S and Ma B: Autophagy and autophagy-related proteins in cancer. *Mol Cancer* 19: 12, 2020.
- Levy JMM, Towers CG and Thorburn A: Targeting autophagy in cancer. *Nat Rev Cancer* 17: 528-542, 2017.
- Kim TW, Lee SY, Kim M, Cheon C and Ko SG: Kaempferol induces autophagic cell death via IRE1-JNK-CHOP pathway and inhibition of G9a in gastric cancer cells. *Cell Death Dis* 9: 875, 2018.
- Zhang G, He J, Ye X, Zhu J, Hu X, Shen M, Ma Y, Mao Z, Song H and Chen F:  $\beta$ -Thujaplicin induces autophagic cell death, apoptosis, and cell cycle arrest through ROS-mediated Akt and p38/ERK MAPK signaling in human hepatocellular carcinoma. *Cell Death Dis* 10: 255, 2019.
- Ramirez JA, Romagnoli GG and Kaneno R: Inhibiting autophagy to prevent drug resistance and improve anti-tumor therapy. *Life Sci* 265: 118745, 2021.
- Mou Y, Wang J, Wu J, He D, Zhang C, Duan C and Li B: Ferroptosis, a new form of cell death: opportunities and challenges in cancer. *J Hematol Oncol* 12: 34, 2019.
- Lou JS, Zhao LP, Huang ZH, Chen XY, Xu JT, Tai WC, Tsim KWK, Chen YT and Xie T: Ginkgetin derived from Ginkgo biloba leaves enhances the therapeutic effect of cisplatin via ferroptosis-mediated disruption of the Nrf2/HO-1 axis in EGFR wild-type non-small-cell lung cancer. *Phytomedicine* 80: 153370, 2021.
- Zhang Y, Tan H, Daniels JD, Zandkarimi F, Liu H, Brown LM, Uchida K, O'Connor OA and Stockwell BR: Imidazole ketone erastin induces ferroptosis and slows tumor growth in a mouse lymphoma model. *Cell Chem Biol* 26: 623-633, 2019.
- Gundala SR, Mukkavilli R, Yang C, Yadav P, Tandon V, Vangala S, Prakash S and Aneja R: Enterohepatic recirculation of bioactive ginger phytochemicals is associated with enhanced tumor growth-inhibitory activity of ginger extract. *Carcinogenesis* 35: 1320-1329, 2014.
- Hong MK, Hu LL, Zhang YX, Xu YL, Liu XY, He PK and Jia YH: 6-Gingerol ameliorates sepsis-induced liver injury through the Nrf2 pathway. *Int Immunopharmacol* 80: 106196, 2020.

19. Xu S, Zhang H, Liu T, Wang Z, Yang W, Hou T, Wang X, He D and Zheng P: 6-Gingerol suppresses tumor cell metastasis by increasing YAP(ser127) phosphorylation in renal cell carcinoma. *J Biochem Mol Toxicol* 35: e22609, 2021.
20. Chen CY, Kao CL and Liu CM: The cancer prevention, anti-inflammatory and anti-oxidation of bioactive phytochemicals targeting the TLR4 signaling pathway. *Int J Mol Sci* 19: 2729, 2018.
21. Liu CM, Kao CL, Tseng YT, Lo YC and Chen CY: Ginger phytochemicals inhibit cell growth and modulate drug resistance factors in docetaxel resistant prostate cancer cell. *Molecules* 22: 1477, 2017.
22. Brahmbhatt M, Gundala SR, Asif G, Shamsi SA and Aneja R: Ginger phytochemicals exhibit synergy to inhibit prostate cancer cell proliferation. *Nutr Cancer* 65: 263-272, 2013.
23. Shukla Y, Prasad S, Tripathi C, Singh M, George J and Kalra N: In vitro and in vivo modulation of testosterone mediated alterations in apoptosis related proteins by [6]-gingerol. *Mol Nutr Food Res* 51: 1492-1502, 2007.
24. Martin SK, Kamelgarn M and Kyriianou N: Cytoskeleton targeting value in prostate cancer treatment. *Am J Clin Exp Urol* 2: 15-26, 2014.
25. Dai SN, Hou AJ, Zhao SM, Chen XM, Huang HT, Chen BH and Kong HL: Ginsenoside Rb1 ameliorates autophagy of hypoxia cardiomyocytes from neonatal rats via AMP-activated protein kinase pathway. *Chin J Integr Med* 25: 521-528, 2019.
26. Ouyang DY, Xu LH, He XH, Zhang YT, Zeng LH, Cai JY and Ren S: Autophagy is differentially induced in prostate cancer LNCaP, DU145 and PC-3 cells via distinct splicing profiles of ATG5. *Autophagy* 9: 20-32, 2013.
27. Li J, Cao F, Yin HL, Huang ZJ, Lin ZT, Mao N, Sun B and Wang G: Ferroptosis: Past, present and future. *Cell Death Dis* 11: 88, 2020.
28. Yan HF, Zou T, Tuo QZ, Xu S, Li H, Belaidi AA and Lei P: Ferroptosis: Mechanisms and links with diseases. *Signal Transduct Target Ther* 6: 49, 2021.
29. Yun DK, Lee J and Keum YS: Finasteride increases the expression of hemoxygenase-1 (HO-1) and NF-E2-related factor-2 (Nrf2) proteins in PC-3 cells: Implication of finasteride-mediated high-grade prostate tumor occurrence. *Biomol Ther (Seoul)* 21: 49-53, 2013.
30. Sp N, Kang DY, Lee JM, Bae SW and Jang KJ: Potential anti-tumor effects of 6-gingerol in p53-dependent mitochondrial apoptosis and inhibition of tumor sphere formation in breast cancer cells. *Int J Mol Sci* 22: 4660, 2021.
31. Radhakrishnan EK, Bava SV, Narayanan SS, Nath LR, Thulasidasan AK, Soniya EV and Anto RJ: [6]-Gingerol induces caspase-dependent apoptosis and prevents PMA-induced proliferation in colon cancer cells by inhibiting MAPK/AP-1 signaling. *PLoS One* 9: e104401, 2014.
32. Kapoor V, Aggarwal S and Das SN: 6-gingerol mediates its anti tumor activities in human oral and cervical cancer cell lines through apoptosis and cell cycle arrest. *Phytother Res* 30: 588-595, 2016.
33. Babaei G, Aziz SG and Jaghi NZZ: EMT, cancer stem cells and autophagy: The three main axes of metastasis. *Biomed Pharmacother* 133: 110909, 2021.
34. Perez TD and Nelson WJ: Cadherin adhesion: Mechanisms and molecular interactions. *Handb Exp Pharmacol* 3-21, 2004.
35. Mendonsa AM, Na TY and Gumbiner BM: E-cadherin in contact inhibition and cancer. *Oncogene* 37: 4769-4780, 2018.
36. Yu W, Yang L, Li T and Zhang Y: Cadherin signaling in cancer: Its functions and role as a therapeutic target. *Front Oncol* 9: 989, 2019.
37. Leggett SE, Hruska AM, Guo M and Wong IY: The epithelial-mesenchymal transition and the cytoskeleton in bioengineered systems. *Cell Commun Signal* 19: 32, 2021.
38. Luo BP, Luo J, Hu YB, Yao XW and Wu FH: Cyclin D1b splice variant promotes alphavbeta3-mediated EMT induced by LPS in breast cancer cells. *Curr Med Sci* 38: 467-472, 2018.
39. Liu T, Zhang J, Li K, Deng L and Wang H: Combination of an autophagy inducer and an autophagy inhibitor: A smarter strategy emerging in cancer therapy. *Front Pharmacol* 11: 408, 2020.
40. El-Khattouti A, Selimovic D, Haikel Y and Hassan M: Crosstalk between apoptosis and autophagy: Molecular mechanisms and therapeutic strategies in cancer. *J Cell Death* 6: 37-55, 2013.
41. Ding Y, Chen X, Liu C, Ge W, Wang Q, Hao X, Wang M, Chen Y and Zhang Q: Identification of a small molecule as inducer of ferroptosis and apoptosis through ubiquitination of GPX4 in triple negative breast cancer cells. *J Hematol Oncol* 14: 19, 2021.
42. Chen P, Wu Q, Feng J, Yan L, Sun Y, Liu S, Xiang Y, Zhang M, Pan T, Chen X, et al: Erianin, a novel dibenzyl compound in Dendrobium extract, inhibits lung cancer cell growth and migration via calcium/calmodulin-dependent ferroptosis. *Signal Transduct Target Ther* 5: 51, 2020.
43. Zhou X, Zou L, Chen W, Yang T, Luo J, Wu K, Shu F, Tan X, Yang Y, Cen S, et al: Flubendazole, FDA-approved anthelmintic, elicits valid antitumor effects by targeting P53 and promoting ferroptosis in castration-resistant prostate cancer. *Pharmacol Res* 164: 105305, 2021.
44. Sun Y, Zheng Y, Wang C and Liu Y: Glutathione depletion induces ferroptosis, autophagy, and premature cell senescence in retinal pigment epithelial cells. *Cell Death Dis* 9: 753, 2018.
45. Rastogi N, Gara RK, Trivedi R, Singh A, Dixit P, Maurya R, Duggal S, Bhatt ML, Singh S and Mishra DP: [6]-Gingerol induced myeloid leukemia cell death is initiated by reactive oxygen species and activation of miR-27b expression. *Free Radic Biol Med* 68: 288-301, 2014.
46. Nigam N, Bhui K, Prasad S, George J and Shukla Y: [6]-Gingerol induces reactive oxygen species regulated mitochondrial cell death pathway in human epidermoid carcinoma A431 cells. *Chem Biol Interact* 181: 77-84, 2009.
47. Mansingh DP, O JS, Sali VK and Vasanthi HR: [6]-Gingerol-induced cell cycle arrest, reactive oxygen species generation, and disruption of mitochondrial membrane potential are associated with apoptosis in human gastric cancer (AGS) cells. *J Biochem Mol Toxicol* 32: e22206, 2018.
48. Xie Y, Hou W, Song X, Yu Y, Huang J, Sun X, Kang R and Tang D: Ferroptosis: process and function. *Cell Death Differ* 23: 369-379, 2016.
49. Salazar M, Rojo AI, Velasco D, de Sagarraga RM and Cuadrado A: Glycogen synthase kinase-3beta inhibits the xenobiotic and antioxidant cell response by direct phosphorylation and nuclear exclusion of the transcription factor Nrf2. *J Biol Chem* 281: 14841-14851, 2006.
50. Abusarah J, Benabdoune H, Shi Q, Lussier B, Martel-Pelletier J, Malo M, Fernandes JC, de Souza FP, Fahmi H and Benderdour M: Elucidating the Role of protandim and [6]-gingerol in protection against osteoarthritis. *J Cell Biochem* 118: 1003-1013, 2017.
51. Wang Q, Wei Q, Yang Q, Cao X, Li Q, Shi F, Tong SS, Feng C, Yu Q, Yu J and Xu X: A novel formulation of [6]-gingerol: Proliposomes with enhanced oral bioavailability and antitumor effect. *Int J Pharm* 535: 308-315, 2018.
52. Adetuyi BO and Farombi EO: 6-Gingerol, an active constituent of ginger, attenuates lipopolysaccharide-induced oxidation, inflammation, cognitive deficits, neuroplasticity, and amyloidogenesis in rat. *J Food Biochem* 45: e13660, 2021.
53. de Lima RMT, Dos Reis AC, de Menezes APM, Santos JVO, Filho J, Ferreira JRO, de Alencar M, da Mata A, Khan IN, Islam A, et al: Protective and therapeutic potential of ginger (*Zingiber officinale*) extract and [6]-gingerol in cancer: A comprehensive review. *Phytother Res* 32: 1885-1907, 2018.



This work is licensed under a Creative Commons Attribution-NonCommercial-NoDerivatives 4.0 International (CC BY-NC-ND 4.0) License.